Proceedings of the ASME 2010 29th International Conference on Ocean, Offshore and Arctic Engineering
OMAE2010
June 6-11, 2010, Shanghai, China

OMAE2010-20009

SUPPORTING NEW INSIGHT IN PIPELINE HYDRODYNAMICS USING STOCHASTIC APPROACHES ON EXTERNAL CORROSION DAMAGE

Zahiraniza Mustaffa*
Section of Hydraulic Engineering
Faculty of Civil Engineering and Geosciences
Delft University of Technology
Delft, The Netherlands.

Civil Engineering Department
Universiti Teknologi PETRONAS
Tronoh, Perak, Malaysia.

Pieter van Gelder
Section of Hydraulic Engineering
Faculty of Civil Engineering and Geosciences
Delft University of Technology
Delft, The Netherlands.

ABSTRACT

Several recent discoveries in the fluid-structure interactions between the external flows and circular cylinders placed close to the wall have added new values to the hydrodynamics of unburied marine pipelines on a seabed. The hydrodynamics of waves and/or currents introduced vortex flows surrounding the pipeline. External corrosions formed in marine pipelines were assumed to be partly contributed by such fluid-structure interactions. The spatial consequences of such interactions were of interest of this study. This paper summarized some experimental and numerical works carried out by previous researchers on these new discoveries. Actual field data were utilized in this study to support this hypothesis. The characteristics of corrosion orientations in the pipelines were studied comprehensively using stochastic approaches and results were discussed. Results adopted from the field data acknowledged well to the hypothesis from the reported literature. The updated knowledge from this fluid-structure interaction is hoped to be given more attention by the industry and perhaps to be incorporated into the current subsea pipeline designs.

1 INTRODUCTION

Two recent works by [1] and [2] have demonstrated the significance of vortex formations surrounding a circular cylinder placed on a wall. This fluid-structure interaction has added values to the hydrodynamics between the flows (waves and/or currents) and pipeline resting on a sea bed. These works, however, were conducted either experimentally or numerically. It has not been proven by actual scenarios as encountered in the pipeline engineering. It is necessary to validate the theory of these new concepts before it can be further explored. This paper is intended to verify the theory from the reported work using actual field data. The hydrodynamics of the fluid-structure interactions were assumed to result in external corrosions on the pipeline wall. The present work which was also a continuation of [3] was carried out using stochastic approaches.

2 FLUID-STRUCTURE INTERACTIONS

Some recent insights on fluid-structure interactions between the external flows (current and/or waves) and unburied pipelines placed in shallow waters are presented in this section. The reported work involved both experimental and numerical, but the review was only restricted to pipelines placed near the sea bed, with vertical distance between the sea bed and the lower part of the pipeline very close to zero. The characteristics of the external flows to the pipelines were critically discussed, and the present work assumed this scenario partly contributed to external corrosions on the pipeline walls.

* Author of correspondence, email Z.B.Mustaffa@tudelft.nl or zahiraniza@petronas.com.my

A structure like pipeline placed in shallow waters behaves under the influence of waves and/or currents. Due to the complexity of the sea floor contours coupled with the interactions between the environmental effects like winds, tides, waves and currents and the shore area, it may be difficult to simply assume the most dominant flow that governs the area of interests. It may be wise in some cases to consider both effects. With this remark, two interesting recent studies on the hydrodynamics of flow around horizontal circular cylinders reported by [1] and [2] were selected for discussions. The work by [1] numerically simulated the wave action on a horizontal circular cylinder using the finite element method. Also computed were the wave force coefficients and velocity fields, and these were later verified with results reported by [4]. Studies by [2] on the other hand, dealt with understanding vortex characteristics exerted by cross flows around a horizontal circular cylinder. Even though both works were looking at the response under different vertical distances between the sea bed and the cylinder, the present study simply chose the scenario when the cylinder was placed close to the sea bed.

These reported work conformed well to the fact that when a horizontal circular cylinder (pipeline) is near the sea bed, the presence of the sea bed changes the symmetric flow. The hydrodynamics of wave and/or current around the pipeline can result in the generation of sheet vortices. A vortex can be seen in the spiraling motion of water around a center of rotation. As the flow moves over the cylinder, the water deforms, rotates, and because of the relatively high velocity, shears and forms a vortex. A group of vortex is called vortices and they contain a lot of energy in the circular motion of the water. These vortices are not stable and shed alternately around the pipeline. The high velocity exerted by the vortex is capable to erode the external surface metal of the pipeline, in which this common scenario is also known as external corrosions.

For pipelines very close to the sea bed, with a given ratio e/D of 0.09, [1] reported that both the wave crest and trout produced vortex flows to the cylinder. [Here e denotes the distance between the sea bed and the lower part of the pipeline and D is the pipe diameter.] They numerically predicted the streamlines at different moments in one wave period, T. From their observations, vortex would form whenever the wave crest and trout passed over the cylinder, even though these happened at different moments in a single T. The locations of these vortices, however, differed from each other, in which the one formed by the wave crest would take place at the downstream section of the cylinder while the other one developed upstream it. Once a vortex formed by the wave crest at t/T=0 s as show in Fig. 1, it would undergo several phases of development accordingly: (i) increased in size and velocity (until t/T=0.25 s), (ii) reduced in velocity, and partially dissipated (t/T=0.33 s), (iii) non-dissipated vortex converted to the upstream, (iv) another vortex formed by wave trout at the upstream section (t/T=0.65 s) and (v) vortex at the downstream section was weaker than downstream due to cancellation effect (t/T=0.8 s).

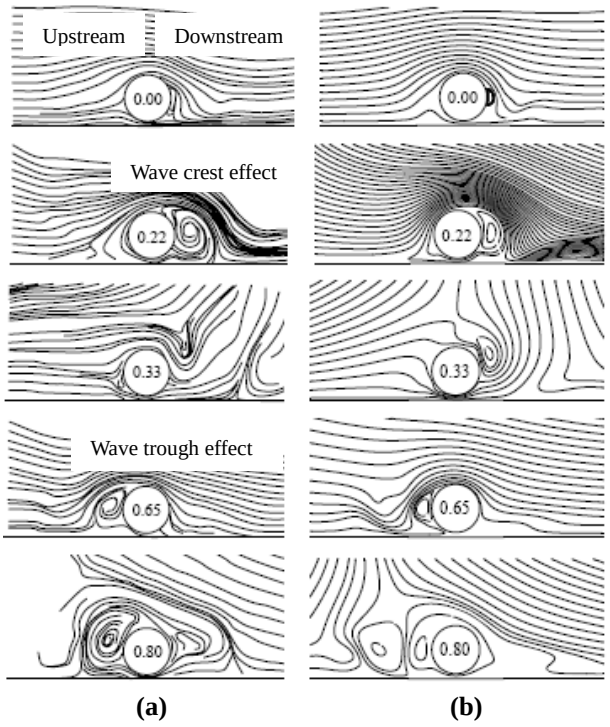

Figure 1. Streamlines near circular cylinder at various values of t/T (shown by the number in the circle) for e/D = 0.1. (a) Numerical work by [1] (b) Experimental work by [4]
(Adapted from [1])

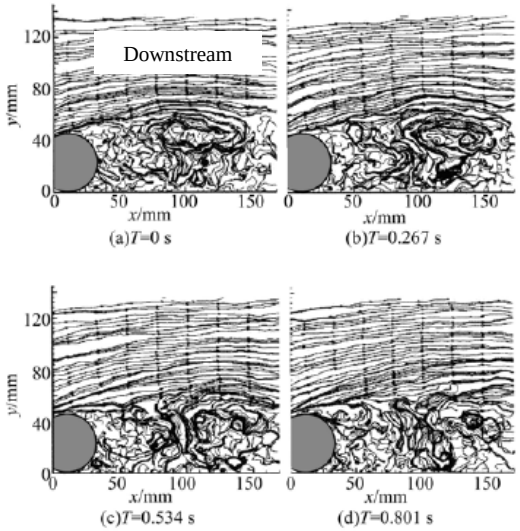

Figure 2. Vortex at downstream section of circular cylinder at e/D=0. (Here T denotes time taken by the *particle image velocimetry* probe to capture images, x and y are the horizontal and vertical distances measured from the cylinder, respectively)
(Adapted from [2])

Due to high velocities in the vortex, the upper part of the cylinder for both upstream and downstream sections was believed to be prone to material loss.

With the aid of a particle image velocimetry probe, similar vortex formation was also visualized by [2]. Since this work only involved cross flows and *e/D* was equal to 0, the location of the vortex was only limited to the downstream section of the cylinder and no flow passed under the cylinder, as can be seen in Fig. 2. This huge vortex has a diameter larger than the cylinder and comprised many small vortices. These vortices, however, were unstable and could instantly move further downstream. Nevertheless, they dissipated with time. Once again it was believed that the upper part of the cylinder at the downstream area which was subjected to vortex activities has high possibility to be exposed to material loss. In the case of a pipeline in particular, corrosions would take place.

The influence of water velocity on early corrosion loss is also briefly discussed here. For this, a work by [5], as shown in Fig. 3 is partly taken for better insights on the matter. [5] summarized contributions to corrosion loss at different water velocities for sea water temperature of 20°C. The higher the velocity, the greater the corrosion loss. This information will be very useful when comparing the plot with the actual current velocity from the case study, which will be presented in Section 3.1 later.

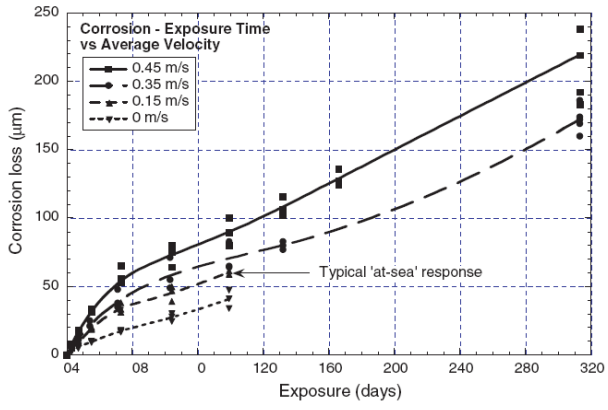

Figure 3. Effect of water velocity on early corrosion loss
(Adapted from [5])

Both the experimental and numerical work discussed earlier have proven the formation of vortex in flows around a cylinder placed close to the sea bed. It is of interest of this present work to represent this scenario from the external corrosions point of view. With this remark, actual field data containing external corrosions in marine pipelines placed on sea bed in shallow water was selected for analysis and discussions. Stochastic approaches were applied to summarize the corrosion characteristics on the external surface of the pipeline.

It is important to highlight here about *similitude* and *scaling* considerations between the two reported work (*i.e.* the models) and present field data (*i.e.* the prototype). If we tried to scale up the expected prototype size and characteristics from the reported work, one would find the values to be overestimated compared to the present field data. Therefore, this paper was not intended to consider the similitude and scaling effects, but rather to predict the spatial consequences that might occur in the prototype by making use of knowledge obtained from the models.

3 CASE STUDY

3.1 Environmental Conditions

This section introduces a case study to represent actual field data for the analysis. A 28" diameter steel pipeline type API 5LX-65 that was 135 km long was selected. The unburied pipeline transported gas from a shallow water of approximately less than 70 m to onshore. The pipeline was installed in 1999 and has been in operation for more than ten years. It can be said that any defects taken place during within this period was more or less stable, with the exclusion of early year defects (resulted from installation *etc.*).

The site was at Kerteh, Terengganu, the east coast of Peninsular Malaysia, about 130 km in the South China Sea (5°50'30"N, 104°07'30"E) as shown in Fig. 4a. The site was a monsoon region, it thus experiences a monsoonal climate created by the influences of the Southwest Monsoon in summer (Fig. 5b) and the Northeast Monsoon in winter (Fig. 5a). The latter is stronger than the former [6]. The typhoons originated from tropical waters far to the east of Peninsular Malaysia and only at rare occasions have they came close to the site [7]. Interested readers are recommended to refer to [6] and [7] for detail descriptions on the environmental conditions of the South China Sea.

Fig. 4b shows the sea bed contour near the pipeline area. According to the 100-year return periods, the given current velocity, significant wave height and periods were 0.36 m/s, 5.3 m and 11.6 s, respectively. Water temperature is measured to be 27°C. The surface current directions within the area is as provided in Fig. 5, and can reasonably applied to this particular site as surface currents are generally restricted to the upper 400 meters of the ocean. Following the description from [6] in the previous paragraph, the dominant current direction would be in winter (Fig. 5a), acting at a cross-flow direction to the pipeline.

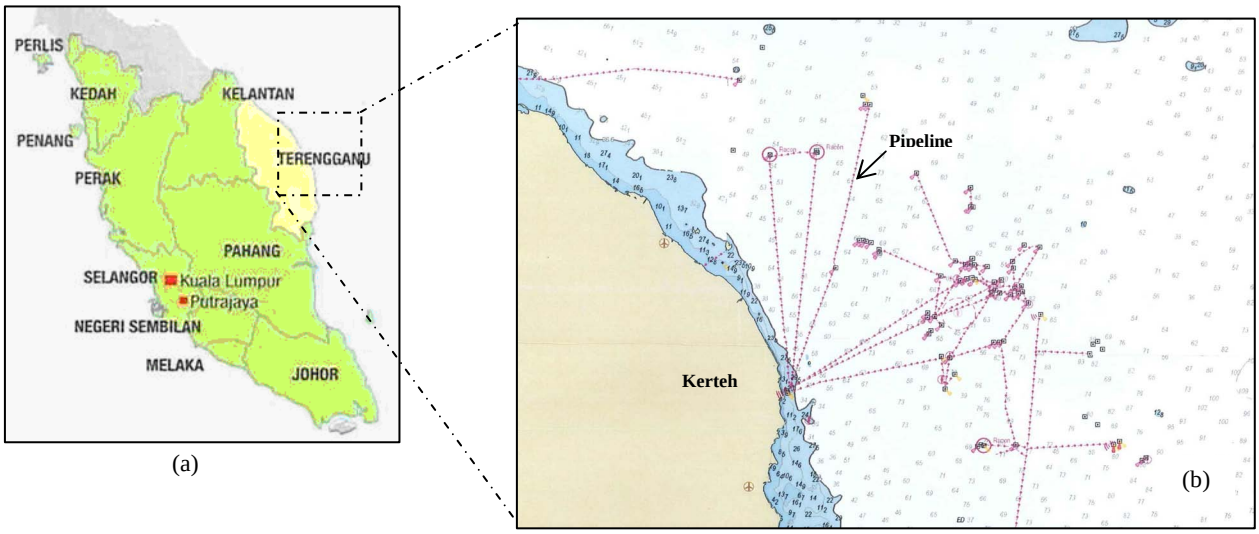

Figure 4. Location of the case study (a) Map of Peninsular Malaysia (b) Part of a hydrographic map showing the shoreline of Kerteh Terengganu, Malaysia and the pipeline tracks

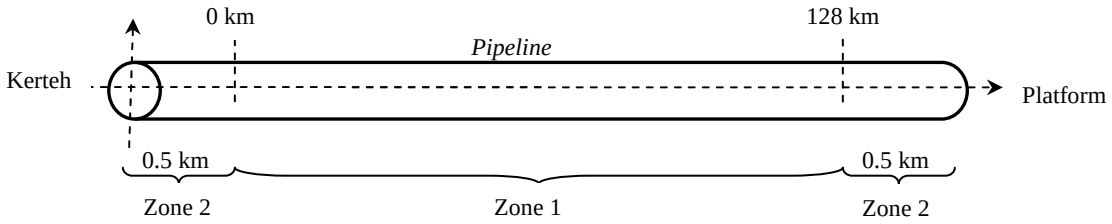

Figure 4c. Longitudinal layout of the pipeline (not to scale)

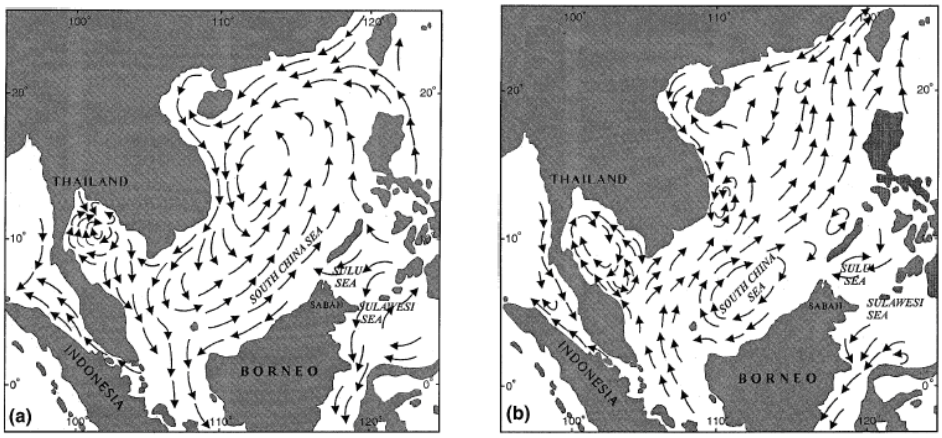

Figure 5. Surface currents of the South China Sea in (a) winter and (b) summer *(Adapted from [7])*

3.2 External Interferences to Pipeline

Several recent reports on the external impacts at the surrounding area of the pipeline were incorporated in the study. It has been reported that the area was free from anchor drags, vessel collisions and dropped objects interferences. The area was not affected by sand erosions as well. No free span exceeding the maximum allowable length was observed. Damaged caused by wave impact *i.e.* splash zone present in the pipeline which mostly taken place in the Zone 2 area near Kerteh (Fig. 4c).

As for the marine habitats, mangroves and seagrass beds were not occupied in the area but coral reefs were more likely to be found in a very shallow water (~15 m). It has not been reported that the area experiencing nutrient pollution caused by the agricultural run-off or sewage pollution in coastal regions and oil pollution at offshore oil fields. These effects, however, have only been investigated qualitatively and the relationship between nutrient levels and increased corrosion has not been quantified [5].

3.3 External Corrosions in Pipeline

307 external corrosion defects of various types were detected in the *Zone 1*(128 km long), as sketched in Fig. 4c. The Zone 1 is an area that excludes 500 m upstream and downstream of the pipeline. It was assumed that this long pipeline has provided sufficient length to the analysis, making some predominant spatial and localized effects like marine growth and sand blasting to be reasonably ignored. Thus the corrosion formations along the pipeline was only subjected to the reactions between the external flows and pipeline surface. The minimum, average and maximum wall loss was 4, 15 and 42%, respectively, calculated with respect to the actual wall thickness. The *intelligent pigging* (*IP*) device used to record corrosion defects in the pipeline gathered comprehensive data on the corrosion defect parameters, represented by the pipeline defect depth, longitudinal length and circumferential width as well as the defects orientation and location. The present work utilized the parameter *defect location* computed by the *IP* in the year 2007 to represent the spatial effects of corrosions. It is also necessary to address here that in spite of *IP* is known to be a source of various uncertainties, it was not of interest of this work to investigate this matter, but to simply acknowledge the results produced by it.

4 DISCUSSION

4.1 Corrosion Distributions along Longitudinal Section of Pipeline

A graphical presentation on the distributions of corrosion defects, particularly the defect depth is presented in Fig. 6-7. The figures revealed that the corrosions were developed almost uniformly throughout the longitudinal length of the pipeline. As mentioned in Section 3.3 earlier, this development pattern was important in order to ensure that the pipeline was almost free from any spatial and localized effects. Despite this assumption, high concentration of defects was observed around the first 20 km distance. Since the water depth in this area was around 15 m deep, it might be partly contributed by the coral reefs as well.

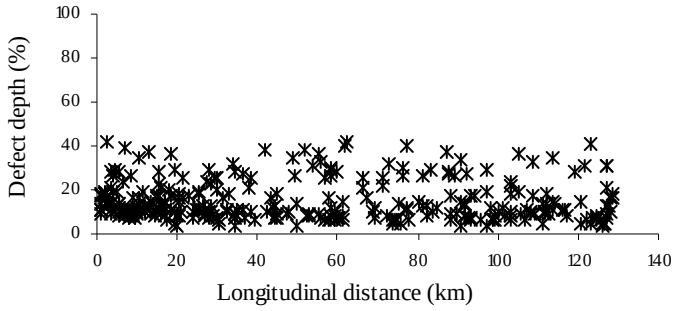

Figure 6. Defect depth along longitudinal distance of pipeline

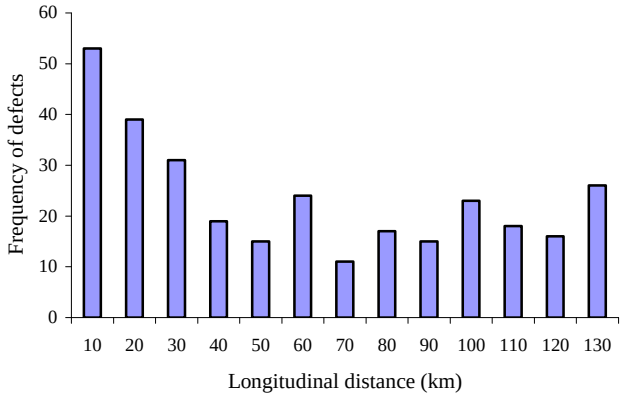

Figure 7. Bar chart showing defect distributions along longitudinal distance of pipeline

4.2 Corrosion Distributions at Cross Section of Pipeline

When uniform corrosion development was assured along the longitudinal pipeline distance, the next step of the analysis was to understand the orientation of each defect with respect to the cross section of the pipeline, as shown in Fig. 8. Also given in the figure was an overview of clock wise orientation, as the *IP* reports each defect with respect to its o'clock position in the pipeline. From here, the corrosions were analyzed according to

their o'clock position and a summary of this can be found in Table 1 and Fig. 9. From these results, it can be clearly seen that high concentration of defects (>20%) were found at 11 and 12, while moderate concentration (>7%) were at 1, 6 and 9 o'clock positions. This hypothesis enables one to conduct proper engineering precautions for those high concentrated locations, but this may not be economical and practical. It may be wise then to further expand the individual o'clock position as a group *i.e.* regions in order to conclude the most dominant location of corrosions.

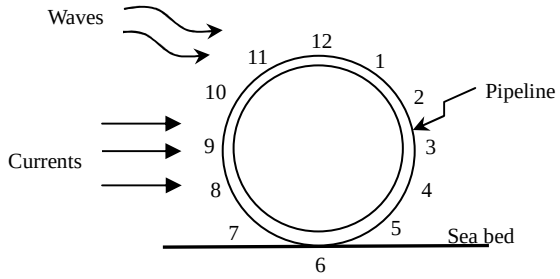

Figure 8. Cross section view of a pipeline, with details of o'clock orientation

Table 1. Number of defects at each o'clock position in the pipeline

O'clock position	1	2	3	4	5	6
Number of defects	26	17	5	16	14	22

O'clock position	7	8	9	10	11	12
Number of defects	16	14	22	25	63	66

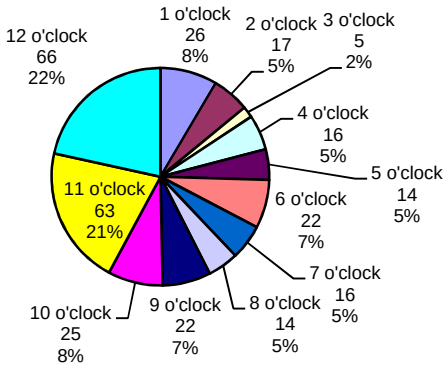

Figure 9. Pie chart on defect distributions at individual o'clock positions

This study introduced one approach to represent the corroded regions. It is important to highlight here that there are various ways to define the regions and this is subjected to many arguments. In this study in particular, the regions were proposed by incorporating the ideologies obtained from the studies of [1] and [2]. The pipeline was subdivided into three unsymmetrical regions, as shown in Fig. 10. Region I was proposed in the area of which corrosions were originated from waves while region II was chosen to determine effects from currents at the downstream section of the pipeline. Region III, however, was not highlighted in the reported works, and simply selected to cater for any sea bed (soil) effects. Region I occupied most of the pipeline area (42%) because the waves reactions as seen from Fig. 1 covered most of the upstream and downstream sections of the pipeline. Also, the size of region II (33%) was made in such a way it would conform to Fig. 2 earlier.

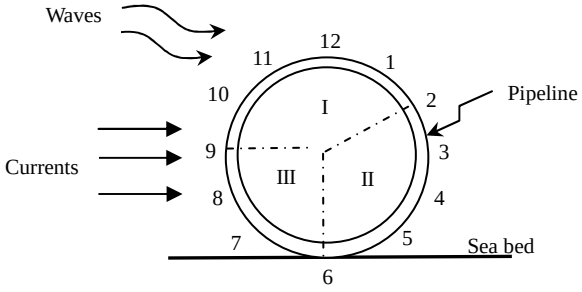

Figure 10. Proposed regions in a pipeline

Table 2. Details of the proposed regions

Region	O'clock positions	Total defects
I	≥ 9, 10, 11, 12, 1, <2	202
II	≥ 2, 3, 4, 5, <6	52
III	≥ 6, 7, 8, <9	52

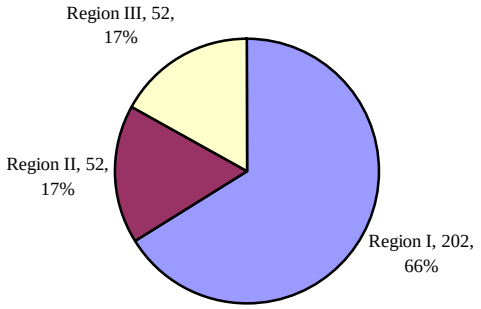

Figure 11. Pie chart on defect distributions at regions

The statistical properties for corrosion distributions in the three regions are as presented in Table 2 and Fig. 11. The results showed that the corrosions were mostly formed in region I, with the highest percentage of 66% and mostly contributed by the 11 and 12 o'clock positions. Even though [1] concluded that vortex (source of corrosions to take place) was visually seen at the downstream and upstream of the pipeline, but for this to take place it needed to travel over the pipeline, thus the 11 and 12 o'clock positions were also prone to be corroded. Therefore, the statistical results of region I can be said in good agreement with the theory of [1]. Region II and III, however, produced similar number of defects (17%). Region II which was hypothetically expected to be subjected to current reactions might be underestimated in this analysis. Despite this underestimation, the characteristics of flow at the downstream part of this pipeline might not be totally dominated by the current because waves also present in the area. Thus careful thoughts and assumptions were needed before comparing any present data with the work by [2]. Region III which was assumed to be governed by the sea bed reactions produced interesting results at the 6 o'clock position. As velocity approaches zero at any walls (*i.e.* sea bed), it was doubt to be able to travel and corrode the 6 o'clock position. Once again, careful thoughts should be given before coming into conclusions for such scenario.

To support the results for the API 5LX-65 pipeline, another pipeline, the API 5LX-60 was selected for comparison. Only 50 external corrosions were detected by the *IP* along a 97 km length. The corrosions distribution for region I in this pipeline is as shown in Fig. 12 below. Results from this figure conformed well to the hypothesis as obtained in the API 5LX-65 pipeline.

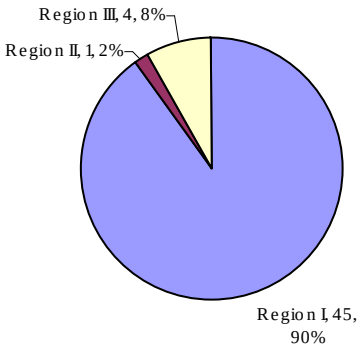

Figure 12. Pie chart on defect distributions at regions for pipeline API 5LX-60

The findings presented in previous paragraphs have led to the investigation of region I for API 5LX-65 pipeline into more details. Two figures are presented to show the distribution of pipeline defects with respect to different o'clock positions in region I, as shown in Fig. 13-14. It can be seen from Fig. 13 that the first 30 km length of the pipeline experienced heavy corrosion activities, while uniform corrosion was almost observed for the remaining part of the pipeline. Fig. 14 reveals the same results as well, with more corrosion contributed by the 11 and 12 o'clock positions at the 30 km upstream. This was likely due to the interactions between waves and the pipeline itself because that area was the closest to the shore. Also noted in Fig 14 was a consistent pattern of corrosions development at the 9, 10 and 1 o'clock positions along the pipeline.

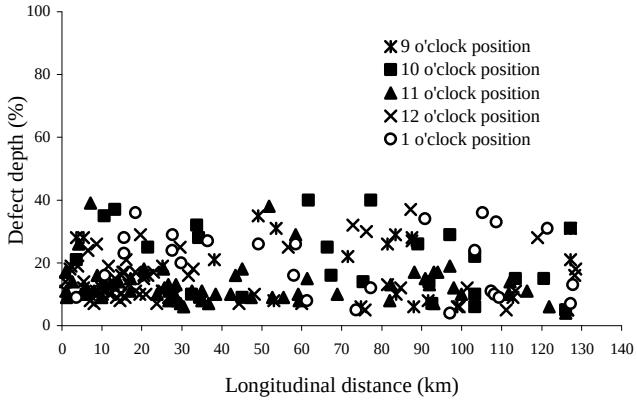

Figure 13. Wall losses for region I of pipeline API 5LX-65

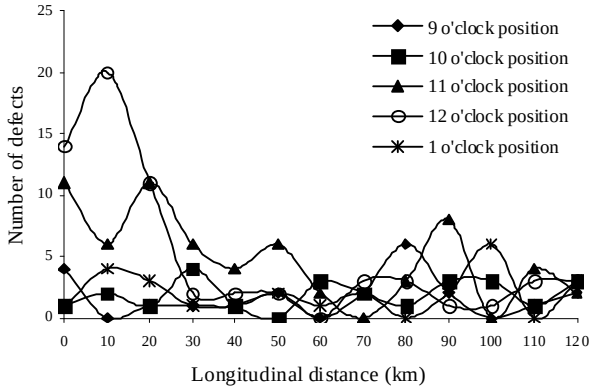

Figure 14. Number of defects for region I of pipeline API 5LX-65

In addition to what has been reported by [1] and [2], the present work revealed two important findings on the spatial consequences of the hydrodynamics activities in region I:

1. Consistent and uniform external corrosions contributed by all o'clock positions.
2. More external corrosions should be expected as the pipeline placed closer to the shoreline, dominated by the 11 and 12 o'clock positions.

4.3 Accurate Identification of Region I

This paper also deliberated about the coverage of circumferential lengths *i.e.* o'clock positions to represent region I which occupied most of the external corrosions. Although there might be many arguments about the selection, the present work tried to utilize the knowledge of stochastic when selecting the boundaries of region I.

The first accuracy check utilized the parameter *number of defects* as an aid for the analysis. The fact that the 11 and 12 o'clock positions comprised more corrosions, these two were then chosen as the middle points for the length. The length was then expanded to the right and left positions with the increment of ±1 o'clock position, both with respect to the middle point mentioned earlier. After doing so, the 10 and 1 o'clock positions were included in the region. From these two positions onwards, the decision for expanding its length was done using simple statistics and expert judgment. For this, Fig. 15 was prepared, summarizing the number of defects occupied in each o'clock position. The figure also provides the average values (μ) of defects at every o'clock interval. It can be seen from the figure that as the position became larger than 2 and smaller than 9 o'clock, the number of defects started to decrease and its mean became smaller than 5. Thus, the boundaries for region I was limited to 9 and 2 o'clock, so that the variation in means compared to the middle points would not be extremely significant (>68%).

Another way of looking at the accuracy check was by applying the parameter *defect depth* at each o'clock position in region I. The variation of corrosion depths along its circumferential length should be able to give some ideas about the spatial effects of the corrosions. In this analysis, another three regions were introduced instead of region I alone, namely *Trials 1, 2* and *3*, as given in Table 3. Also given in the table is the o'clock positions governing each trial regions. The analysis was carried out by choosing the best fit probability density function (pdf) for the corrosion depth data. This was done by using a statistical software called *BestFit*. The pdf that suited the data the most and its corresponding statistical parameters *mean*, *standard deviation*, *skewness* and *kurtosis* are also provided in Table 3. The mean describes the average value of a sample data and the standard deviation is a measure of the variability or dispersion of the data with respect to the mean. The skewness is a measure of symmetry while the kurtosis tells whether the data are peaked or flat relative to a normal distribution. Interested readers are advised to refer to several basic statistics and probabilistic books for further understanding about this matter.

These four parameters were able to judge the characteristics of defect depths distribution in all the regions given in Table 3. The answer that one would be interested to find is lower values of standard deviation, skewness and kurtosis. Nevertheless, it was difficult to distinguish such pattern for the statistical results presented in Table 3. It was then evaluated on a case-by-case basis. Region I was larger than trial II by 1 o'clock position. Even though with the smaller area, trial II produced higher skewness and kurtosis, so its less data have provided infrequent extreme deviations to the sample. On the hand, even though the standard deviation for trial I was smaller than region I, its area of coverage was small and this might exclude the dominant wave reactions at the upstream section of the pipeline. The lower values of skewness and kurtosis in trial III were favorable, but its large area might overestimate the current interactions at the downstream section of the pipeline.

Despite totally relying on stochastic approaches, care should be taken not to neglect the hypothesis of [1] and [2] earlier. As long as the theories were assured the selection of final boundaries would be acceptable.

CONCLUSIONS

The present study utilized actual field data to validate earlier theoretical (experimental and numerical) works on fluid-structure interactions between external flows (waves and/or currents) and circular cylinders (pipelines). The hydrodynamics of vortex flows produced in the fluid-structure interactions were assumed to result in external corrosions on the pipeline walls. This work critically analyzed the spatial consequences of corrosions by considering the defect orientations measured from the cross section of the pipeline. It was proposed to describe the corrosions distributions by regions, instead of analyzing it individually. The accuracy of the circumferential length covered by the proposed region was conducted by means of stochastic approaches and expert judgments.

Results from this study conformed well to theories for pipelines under the waves effects, but careful considerations should be taken when dealing with pipelines dominated by currents. Nevertheless, other external influences that might contribute to corrosions should also be taken into account.

Two new values were added to this fluid-structure interaction in the proposed region, it was found that (i) each o'clock position would have consistent and uniform corrosions development, but (ii) more corrosions should be expected as the pipeline placed closer to the shoreline, which was mainly dominated by the 11 and 12 o'clock positions.

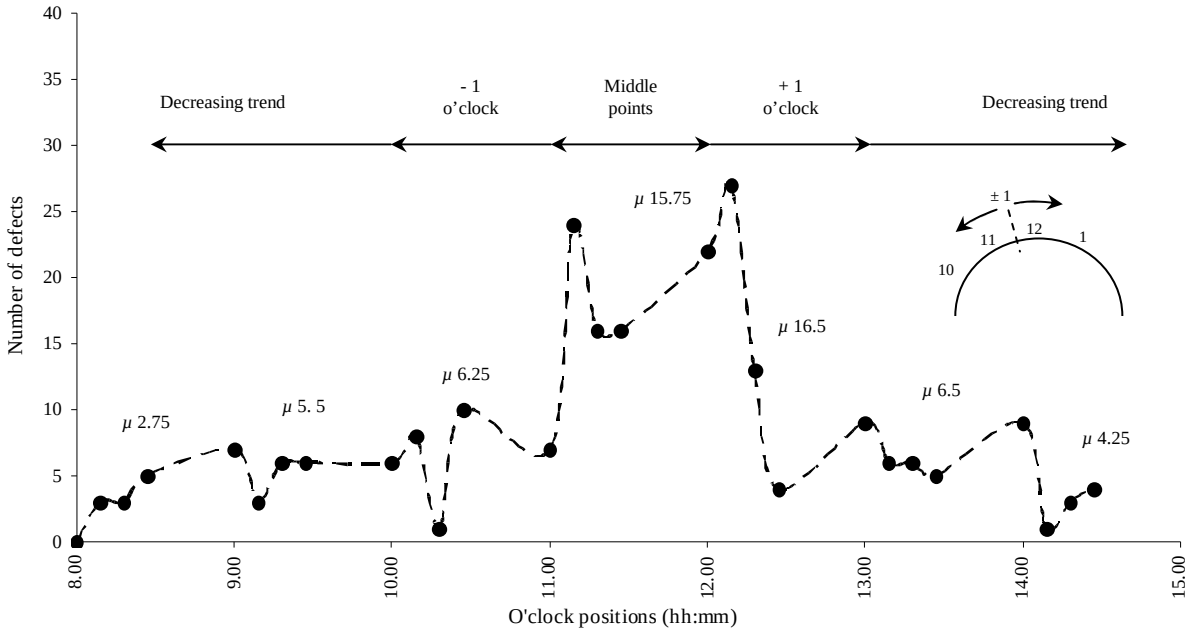

Figure 15. Number of defects with respect to its cross section for region I

Table 3. Details of Trial 1, 2 and 3

Regions	Coverage area	Pdf	Mean	Standard deviation	Skewness	Kurtosis
Region I (≥ 9, 10, 11, 12, 1, <2)	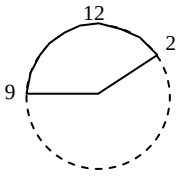	Lognormal2	15.95	8.75	0.95	2.95
Trial I (≥ 10, 11, 12, 1, <2)	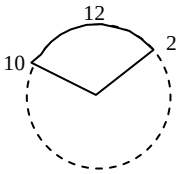	Lognormal	15.52	8.55	1.12	3.43
Trial II (≥ 9, 10, 11, 12, <1)	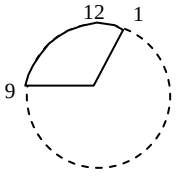	Lognormal2	15.38	8.39	1.13	3.50
Trial III (≥ 9, 10, 11, 12, 1, 2, <3)	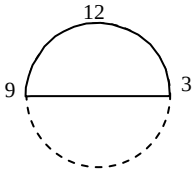	Lognormal2	15.79	8.73	0.97	3.13

The present work may be further expanded by analyzing a few more pipeline candidates in order to avoid ambiguities in the dominant external flows acting on the pipelines. The analysis shall be able to distinguish the hydrodynamic effects under waves, currents and when both acting together.

ACKNOWLEDGMENTS

The authors would like to thank Petroliam Nasional Berhad (PETRONAS), Malaysia for providing data for this project, which was financed by the Universiti Teknologi PETRONAS, Malaysia and Schlumberger Foundation. Also, special thanks to Teh Hee Min from University of Edinburgh for his technical advice on the preliminary stage of this study.

REFERENCES

[1] Zhao, M., Cheng, L. and Ah, H., 2006, "A Finite Element Solution of Wave Forces on a Horizontal Circular Cylinder Close to the Sea-Bed", *Journal of Hydrodynamics*, Ser. B, Vol. 18, Issue 3, Supplement 1, pp 139-145.

[2] Qi, E.R., Li, G. Y., Li, W. and Wu, J., 2006, "Study of Vortex Characteristics of the Flow around a Horizontal Circular Cylinder at Various Gap-Ratios in the Cross-Flow", *Journal of Hydrodynamics*, Ser. B, Vol. 18, Issue 3, Supplement 1, pp 334-340.

[3] Mustaffa, Z, van Gelder, P.H.A.J.M., and Vrijling, J. K., 2009, "A Discussion of Deterministic vs. Probabilistic Method in Assessing Marine Pipeline Corrosions", *The 19th International Offshore and Polar Engineering Conference (ISOPE*) , Vol. 4, pp 653-658.

[4] Jarno-Druaux, A., Sakout, A., and Lambert, E. , 1995, "Interference between a circular cylinder and a plane wall under waves", *Journal of Fluids and Structures*, No. 9. pp 215–230.

[5] Melchers, R. E., 2005, "The Effect of Corrosion on the Structural Reliability of Steel Offshore Structures", *Corrosion Science*, No. 47, pp 239-2410.

[6] Morton, B., and Blackmore, G., 2001, "South China Sea", *Marine Pollution Bulletin*, Vol. 42, No. 12, pp 1236-1263.

[7] Brink-Kjaer, O., Kej, A. and Pushparatnam, E., 1986, "Environmental Conditions in the South China Sea Offshore Malaysia: Hindcast Study Approach", *Offshore Technology Conference*, OTC 5210, pp 477-483.

[8] Tuen, K. L., 1994, "Monitoring of Sea Surface Temperature in the South China Sea", *Hydrobiologia*, No. 285, pp 1-5.

[9] Chakrabarti, S. K., 1994, "*Offshore Structure Modeling*", *Advanced Series on Ocean Engineering – Volume 9*, World Scientific, p 470.